

A STAR PATTERN RECOGNITION ALGORITHM FOR AUTONOMOUS ATTITUDE DETERMINATION

R. W. H. van Bezooijen

*Guidance and Control Section, Jet Propulsion Laboratory,
California Institute of Technology, Pasadena, CA 91109, USA*

Abstract. A star pattern recognition algorithm is described enabling a state-of-the-art star tracker to quickly and reliably determine its attitude about all three axes without requiring any a-priori attitude knowledge. This device, referred to as a "Full-sky Autonomous Star Tracker (FAST)," can serve as a key sensor in future autonomous attitude control and navigation systems. Having a field of view of 11.5 by 11.5 degrees and an accuracy of 8 arcsec (1 sigma), the redundant, microcomputer equipped ASTROS II star tracker being developed by JPL for use with the Mariner Mark II planetary spacecraft is ideally suited to serve as a FAST. It is shown that an ASTROS II based FAST, integrated with an all-sky database of some 4,100 guide stars, and 810K bytes of memory, can determine its attitude in approximately 1 second with a success rate very close to 100%. Its high speed is due to both the accuracy of the tracker and the efficiency of the algorithm which usually does not require any iterations.

In addition to enabling a FAST, the recognition algorithm can also be used for automating the acquisition of celestial targets by astronomy telescopes, for updating the attitude of gyro based attitude control systems autonomously (planned for Mariner Mark II), and for automating ground based attitude reconstruction. Monte Carlo simulations and a much faster, highly accurate quasi-analytical method are used for predicting the success rate of the algorithm as a function of the many parameters required to define the sky, the star catalog from which the guide stars are extracted, the tracker, and the control parameters of the algorithm.

Keywords. Pattern recognition; attitude control; autonomous systems; space vehicles; tracking systems.

INTRODUCTION

The purpose of this paper is to describe a robust, nominally non-iterative star pattern recognition algorithm, enabling fast autonomous attitude determination. Although not restricted to, the algorithm is intended for use with star trackers (STRs) equipped with two-dimensional solid state array detectors capable of accurately measuring the position and brightness of multiple stars within the field of view (FOV). The algorithm has a wide range of applicability. It can be used for automating the acquisition of celestial targets by astronomy telescopes, for autonomous updating of gyro-based attitude control systems, and for ground-based attitude reconstruction. Most interestingly, the recognition algorithm enables the construction of a Full-sky Autonomous Star Tracker (FAST), capable of accurately determining its attitude about all three axes without requiring any a-priori attitude knowledge.

The attitude determination problem requiring star pattern recognition is illustrated in Fig. 1. Due to attitude errors, the coordinate system associated with the star tracker (X_o, Y_o, Z_o) deviates from its expected inertial orientation (X_i, Y_i, Z_i). Employing geometric and brightness criteria, a star pattern recognition algorithm is used to determine which of the stars observed by the tracker (the "observed stars") correspond to which of the a-priori selected "guide stars". If at least two of the observed stars are guide stars, and these stars are correctly identified, the attitude about all three axes (angles α , β , and γ) can be computed. The area in which the guide stars are selected, referred to as the "uncertainty area," needs to be sufficiently large to ensure that it will include the field of view of the star tracker. In the case of FAST, the uncertainty area covers the entire sky. As is illustrated by Fig. 1, some of the guide stars within the FOV of the STR may not be observable, while some of the observed stars may be non-guide stars. The recognition algorithm needs to be sufficiently robust to cope with this situation.

The performance of the star pattern recognition algorithm has been tested using two very different cases. The first case involves use of the algorithm for the autonomous acquisition of celestial targets by the Space Infra Red Telescope Facility

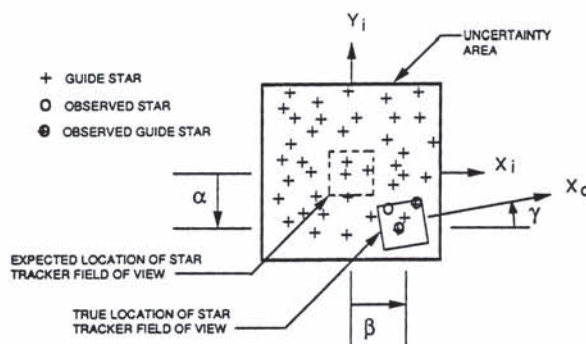


Fig. 1. Attitude Determination Problem.

(SIRTF). The second test case pertains to the situation where the algorithm is used as an integral part of a FAST. The number of guide stars required per attitude determination is typically less than 100 for SIRTF, while for the FAST it is in excess of 4,000.

SIRTF (Eisenhardt and Fazio, 1988), will be a spacecraft carrying a 1-m class cryogenically cooled infrared telescope nearly three orders of magnitude more sensitive than the current generation of infrared telescopes. The primary attitude data used for pointing SIRTF will be provided by a Charge-Coupled Device (CCD) STR having a 15 arcmin diameter FOV. To ensure sufficient alignment stability, the STR will be integrated in the detector bay of the telescope as is shown in Fig. 2, where it is referred to as the Fine Guidance Sensor. Because of its small FOV, use of guide stars up to magnitude 15 is required. These stars can be extracted from the catalog prepared for the Hubble Space Telescope (Lasker, Jenker, and Russell, 1987).

Following each slew to a new target, the recognition algorithm is used for identifying the observed stars, thus permitting determination of the attitude (angles α , β , and γ in Fig. 1). After having established its attitude, SIRTF is rotated to its desired pointing attitude where the stars used for pointing

control are acquired. Because of the small value of the post-slew attitude error (expected to be less than 5 arcmin per axis, 1 sigma), a special star pattern recognition algorithm, described by van Bezooijen, Lorell, and Powell (1985), can be used for SIRTf, instead of the general algorithm described in this paper. This special algorithm, which is a subset of the general algorithm, allows an important reduction of the memory space required.

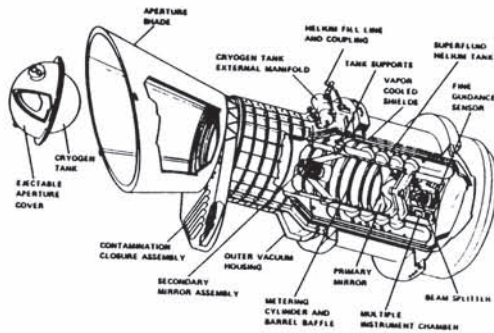


Fig. 2. Telescope of the Space Infra Red Telescope Facility (SIRTf) with the Star Tracker (Fine Guidance Sensor).

Applied to SIRTf, the success rates of the special and general recognition algorithms were established using Monte Carlo simulations. Since all failed cases can be diagnosed, the simulations are very important for developing and perfecting recognition algorithms. However, in order to obtain sufficient statistical confidence, it is necessary to perform many evaluations (typically at least 1000 per case), requiring very long compute times. This motivated the development of a quasi-analytical method, described in detail by van Bezooijen (1986), for obtaining the recognition success probability. The quasi-analytical method, which is typically two to three orders of magnitude faster, yields results that closely match the values obtained with the simulations.

The FAST, used as the second test case for evaluating the performance of the general recognition algorithm, is based on the redundant ASTROS II CCD star tracker (Dennison, Stanton, and Shimada, 1987), being developed by JPL for use with the Mariner Mark II planetary spacecraft (Draper, 1988). Having a FOV of 11.5 by 11.5 degrees and a spatial accuracy of 8 arcsec (1 sigma, goal), ASTROS II is ideally suited to serve as a FAST. Its large FOV allows the number of guide stars in the database of the tracker to be limited to a manageable number, while its high accuracy ensures that the pattern formed by the observed guide stars is unique. Furthermore, this tracker is integrated with a redundant radiation-hard microcomputer capable of performing the star identification in approximately one second.

PREVIOUS RELATED RESULTS

In the past, primitive versions of automated star identification have been used onboard spacecraft. The identification process was simple, involving only a few guide stars per attitude determination. Planetary spacecraft typically used Canopus as a single guide star. Being the brightest star in the area searched, identification of Canopus is fairly simple. The Astronomical Netherlands Satellite (ANS), used guide star pairs for acquiring celestial targets (Christis, 1974). The Infra Red Astronomical Satellite (IRAS), used a redundant V-slit type star sensor in the focal plane of the telescope for updating its attitude (McLaughlin and de Leeuw, 1978; van Bezooijen, 1977). The number of guide stars used per update was selectable and could vary from 1 to 5. For the foregoing three examples, one component of the pointing error of the star sensor was kept very small by using a sun sensor.

Galileo (Rhoads Stephenson, 1985) will use a V-slit type star sensor mounted on the spinning part of the dual-spin spacecraft. Although use of an onboard all-sky guide star catalog was initially planned (Wong and Breckenridge, 1983), memory limitations necessitated a vast reduction of the number of guide stars. It is now planned to typically use 6 guide stars for a particular orientation of the spin axis. A star identification

method utilizing CCD trackers has been described by Junkins and Strikwerda (1979). Their method is iterative and is based on matching pairs of observed stars with pairs of guide stars. Its application is limited to cases where the attitude error is small relative to the FOV of the tracker.

RECOGNITION ALGORITHM

Overview

The objective of the recognition algorithm is to find the largest group of observed stars that matches a group of guide stars. The "basic" recognition algorithm assumes that a group of observed stars matches a group of guide stars if all of the following criteria are met:

1. The measured angular distance of each pair of observed stars matches the predicted angular distance of the corresponding pair of guide stars to within the distance tolerance (*tdis*).
2. The measured magnitude of each of the observed stars matches the predicted magnitude of the corresponding guide stars to within the magnitude tolerance (*mag*).
3. The geometry of the group of observed stars is not the mirror image of that of the corresponding group of guide stars.

In the above, the angular distance of a star pair is defined as the angle between the two stars of the pair. It is usually convenient to use the "vector distance" between two stars as a measure of the angular distance. The vector distance is defined as the linear distance between the stars, assuming that the stars are located on a celestial sphere with unit radius.

It may be seen that the basic algorithm exploits the full information contents of the pattern, thereby maximizing the recognition success rate. Or, in other words, the algorithm performs checks on all independent variables defining a pattern.

If the attitude error is small, as is true for SIRTf, an additional "rotational" criterion is imposed. This criterion states that the rotation angle of the tracker about the boresight (angle γ in Fig. 1) needed to align the pattern of observed stars with the pattern of guide stars is less than the FOV rotation tolerance (*tro*).

The star pattern recognition process consists of the following steps:

1. Generation of match groups through star pair matching
2. Elimination of small match groups that are likely to be spurious
3. Validation of the remaining match groups
4. Elimination of redundant valid match groups
5. Extraction of the largest valid match group(s)

A match group consists of a kernel star match plus a number of associated star matches. Each star match in a match group links an observed star with a guide star. Fig. 3 shows an example of a match group. The group consists of four star matches, the kernel consisting of a match of observed star 1 and guide star 14, and three associated star matches. The group was created because the star pair consisting of guide stars 14 and 26 matched the star pair consisting of observed stars 1 and 2, guide star pair 14, 51 matched observed star pair 1, 4, and guide star pair 14, 3 matched observed star pair 1, 7. In the example of Fig. 3, three different star pair matches have indicated that observed star 1 may be guide star 14, and the match group is assigned a "match confirmation value" of 3. Validation of the match group shown in Fig. 3 involves checking if the three remaining angular distances (indicated by broken lines in Fig. 4) do match.

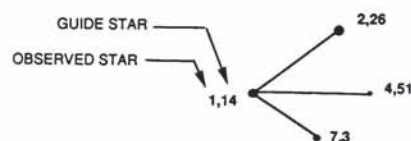


Fig. 3. Match Group Example.

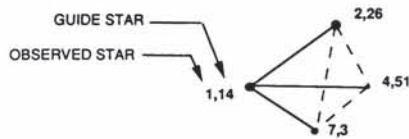


Fig. 4. Example of Match Group Validation.

Usually, only one match group remains following execution of step 5, in which case the recognition process is completed. If two or more match groups remain, and all remaining groups have at least two star matches in common, the recognition process is also completed. In the latter case, it is assumed that more than one group remained due to the fact that one of the observed guide stars had a particularly large position error as will be explained in the next section. In all other cases, it is assumed that no solution was found because the threshold used for elimination of small match groups was too high, and steps 2 through 5 are repeated using a lower threshold.

If, even after successive threshold reductions, no result is obtained, the algorithm can switch to a mode where the initial threshold value is restored and steps 2 through 5 are repeated. In this mode, ambiguity (more than one match group after step 5) is resolved by selecting the best match group (see next section for quality criterion).

From the above, it may be seen that the recognition process is usually non-iterative, making it very fast. Iterations, if required, are very fast due to the fact that the match information generated in step 1 is always saved, while the time required for execution of steps 2 through 5 is very small compared to that of step 1.

Algorithm Description

A high level flow diagram of the general recognition algorithm is shown in Fig. 5. The four operations between the first and second if statements (diamonds) perform steps 1 through 5 mentioned in the previous section. Step 1 is performed by the first operation, while steps 2 through 5 are performed by the fourth operation. The parameters LOOP (initialized at 0) and ISWPR determine if the best match group is to be selected in case of ambiguity. If we want to use this option, ISWPR needs to be set to a value different from 1. The LOOP parameter is required to ensure that ambiguity resolution will be used only if successive threshold reductions yield no solution.

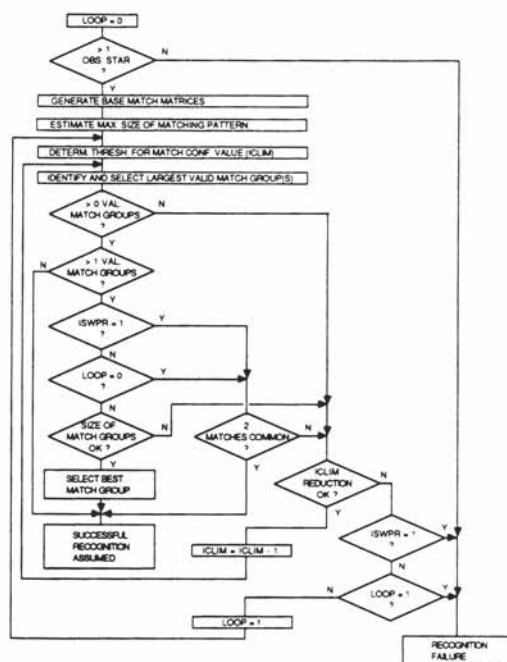


Fig. 5. High Level Flow Diagram of the Recognition Algorithm.

If there is only 1 observed star, something that can happen due to the dynamic range limitation of the tracker, the recognition fails due to the fact that this star is unlikely to be unique, while, if it were unique, it would not allow three axis attitude determination.

If there are two or more observed stars, a list of match groups will be generated using star pair matching. This process starts by identifying all guide star pairs in the uncertainty area having an angular distance less than the largest dimension of the STR FOV (diameter or diagonal). In the case of FAST, all guide star pairs have been identified a-priori and are stored in the memory of the tracker in sequence of increasing angular distance. The latter is done to make the search for matching guide star pairs as fast as possible. Next, it is determined which pairs of guide stars match each pair of observed stars. A star pair match occurs if all of the following conditions are satisfied:

1. The angular distance of the guide star pair differs less than $tdis$ from that of the observed star pair.
2. The rotation about the boresight of the STR needed to align the guide star pair with the observed star pair is less than $trot$.
3. Each guide star of the pair has a predicted instrument magnitude that differs less than mag from that of the corresponding observed star.

Obviously, condition 2, which is important in cases where the attitude error is small (e.g., SIRTf), is not enforced in the case of FAST. Following the detection of a match, the list of match groups is updated.

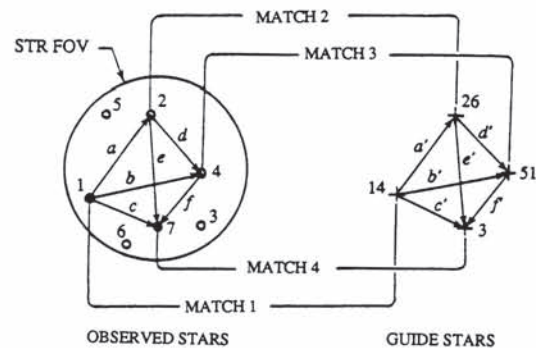


Fig. 6. Star Match Example (Four of the Observed Stars are Guide Stars).

This process is illustrated using Fig. 6 which shows a situation where four (stars 1, 2, 4, and 7) of the seven observed stars are guide stars (stars 14, 26, 51, and 3 respectively).

If the six observed star pairs a through f are the first ones to be evaluated out of a total of 21, and the evaluation is done in that sequence, then the first four resulting match groups are the ones shown in Table 1. Following the match of guide star pair a' with observed star pair a , the match of observed star 1 with guide star 14 is designated match 1, while that of observed star 2 with guide star 26 is designated match 2. Table 2 shows how each star match (i) is linked to an observed star, $OMAT(i)$, and a guide star, $GMAT(i)$. In addition, match group 1 is created with match 1 as its kernel ($KMAT(1) = 1$), and match 2 as the first match associated with this kernel ($MAT(1,1) = 2$). The confirmation value of the match group is set to 1 ($NASS(1) = 1$). Similarly, the second match group is created with match 2 as its kernel, match 1 as its first associate match, and a confirmation value of 1. After matching b' with b , the third match is defined ($OMAT(3) = 4$ & $GMAT(3) = 51$), the third match group is created with match 3 as its kernel and match 1 as its first associate and a confirmation value of 1. Further, match group 1 is updated by adding a second associate match ($MAT(1,2) = 3$) and raising its confirmation value to 2. After the last match of f with f' , the first four lines of the list of match groups has been created.

Due to coincidence star pair matches, there will usually be many more match groups, while the first four match groups may have spurious associated matches and thus greater

confirmation values. In the case of FAST, there will typically be some 5000 false match groups. All information of the match groups is contained in the vectors $KMAT(ig)$, $NASS(ig)$, $OMAT(i)$, $GMAT(i)$, and the matrix $MAT(ig,j)$, where ig refers to the match group. This set of matrices is referred to as the base match matrices. If pair b' does not match pair b , the base match matrices are different as is indicated by the numbers within parentheses in Table 1.

TABLE 1 Example of List of Match Groups

Match Group	Kernel Match	Confirmation Value	Matches Associated with Kernel		
			First	Second	Third
<i>ig</i>	$KMAT(ig)$	$NASS(ig)$	$MAT(ig,1)$	$MAT(ig,2)$	$MAT(ig,3)$
1	1	3 (2)	2 (2)	3 (4)	4 (-)
2	2	3 (3)	1 (1)	3 (3)	4 (4)
3	3	3 (2)	1 (2)	2 (4)	4 (-)
4	4	3 (2)	1 (1)	2 (2)	3 (3)

Note: The numbers within parentheses are for $b \neq b'$ (see Fig. 6)

TABLE 2 Example of Matched Observed and Guide Stars

Match Number	Observed Star	Guide Star
<i>i</i>	$OMAT(i)$	$GMAT(i)$
1	1	14
2	2	26
3	4	51
4	7	3

Next, the maximum size of a match group is estimated by noting that in order to have a group with n star matches, there need to be at least n match groups with a confirmation value of at least $n-1$ each. Having found the maximum size (e.g., n), a threshold (ICLIM) is defined that is initially set to $n-1$ -ICMAXR, where ICMAXR is a control parameter that needs to be at least 1. Using the threshold, all match groups having a confirmation value equal or less than the threshold are eliminated as they are suspected to be spurious. Furthermore, the remaining match groups are adjusted to account for any associated matches that were kernels of eliminated match groups.

In the following step, the remaining match groups are validated by imposing a geometry test, where it is checked if the angular distance of all observed star pairs of the group matches that of the corresponding pair of guide stars. For match group 1 in the example (shown in Fig. 3), which has associated matches 2, 3, and 4, it implies that the distances associated with match 2 & match 3, match 2 & match 4, and match 3 & match 4 are checked (indicated by broken lines in Fig. 4). The first of these three tests is executed by checking if match $MAT(1,2)$, = match 3, is an associate star match of the kernel of match group $MAT(1,1)$, = match group 2, which is indeed the case. This process is continued until it has been verified that the remaining three distances of match group 1 do match.

The geometry test is finalized by checking if the pattern of guide stars is not the mirror image of the pattern of observed stars. This is done by verifying that the signs of the vector product of a and b and that of a' and b' are the same. If all distances match, the end result of the geometry test is shown in Table 3, case a. If distance b differs from b' by more than $tdis$, then the end result would be as case c of Table 3. Because b was found not to match b' , match group 2 split into two match groups, 2a with matches 1 & 4, and 2b with matches 3 & 4. The same happened to match group 4.

As the possibility exists that two angular distances do not match because of a "high sigma case" for the position of one of the two guide stars involved, and it is noted that the recognition success probability drops with a reduction of the number of

stars in the pattern, a "relaxed distance tolerance" $tdisl$ ($tdisl > tdis$) can be specified for the match group validation process. If the difference between b and b' were less than this tolerance, the match groups shown as case b in Table 3 would result. Otherwise, the groups shown as case c would be generated.

TABLE 3 Match Groups Passing Geometrical Tests

Case	Match Group	Kernel Match	Confirmation Value	Matches Associated with Kernel		
				First	Second	Third
a	1	1	3	2	3	4
	2	2	3	1	3	4
	3	3	3	1	2	4
	4	4	3	1	2	3
b	1	1	2	2	4	-
	2	2	3	1	3	4
	3	3	2	2	4	-
	4	4	3	1	2	3
c	1	1	2	2	4	-
	2a	2	2	1	4	-
	2b	2	2	3	4	-
	3	3	2	2	4	-
	4a	4	2	1	2	-
	4b	4	2	2	3	-

Next, redundant match groups are eliminated, implying that one group is left in case a of Table 3, two in case b, and two in case c. This is followed by extraction of the largest remaining match group(s). Usually, there is only one match group left at this point, and the matches of this group are assumed to be correct. If there are two or more match groups left, and these groups have at least two star matches in common (see case c), then successful recognition is also assumed.

If there is no remaining match group, or multiple groups were found without common star matches, then it is assumed that the threshold ICLIM was set too conservatively and the process is repeated after decrementing the threshold. If this yields no solution after having lowered the threshold to its minimum value, and the control switch ISWPR was set to 1, the algorithm reports that it cannot perform the recognition. However, if ISWPR had been set to any other value, a second recognition attempt is performed upon having set the LOOP parameter to 1 (initialized at 0).

If during this second attempt the situation is encountered where there is more than one remaining match groups, the match group with the highest quality is selected and the algorithm assumes the recognition to be successful. The sum of the differences between the angular distances of the observed star pairs and the corresponding guide star pairs is used as the quality index. The group with the lowest index is assumed to contain the correct matches.

Having identified the stars, a least squares solution can be used for determining the attitude of the tracker.

Special Algorithm

If the attitude error is small (requiring an uncertainty area of typically 10 times the area of the tracker FOV), as is the case for SIRTf, a less complex algorithm, referred to as the "special algorithm," can be applied. This algorithm finds the largest group of observed stars that can be "matched" with a group of guide stars by rotating the tracker over angles α and β from its expected orientation (see Fig. 1).

Star pair matching is used to generate a "match matrix". This matrix has a row for each observed guide star used for recognition and a column for each guide star. Each time a guide star pair is found to match an observed star pair, the appropriate two elements of the matrix (initialized at zero) are incremented by one, implying that the value of the matrix elements corresponds to the confirmation value.

Using the example of Fig. 6 again, the star pair matching would ideally result in a match matrix having values of 3 for the matrix elements (1,14), (2,26), (4,51), and (7,3) and values of zero for all other remaining elements. However, due to coincidence star pair matches, the aforementioned four matrix elements may have values in excess of 3, while many other elements may have values greater than zero.

In the next step, the low value matrix elements are eliminated and the pointing error (angles α and β in Fig. 1) associated with each of the remaining matrix elements is established, assuming zero FOV rotation error ($\gamma = 0$). The largest group of star matches having "equal" α and β values (allowing for differences consistent with the FOV rotation tolerance) is then assumed to represent the correct matches of guide stars with observed stars.

SUCCESS RATE OF RECOGNITION ALGORITHM

Test Cases and Evaluation Methods

The general star pattern algorithm is evaluated for two extreme test cases, SIRTf with its 15 arcmin diameter STR FOV, and a FAST with a 100 square degree circular FOV (11.3 degree diameter). For SIRTf, both the general and special algorithms were evaluated using Monte Carlo simulations. These simulations were also utilized for improving the general algorithm. Because of the ability to output diagnostics, Monte Carlo simulations are an essential tool for developing and refining recognition algorithms. However, the method requires a large number of evaluations per case in order to obtain sufficient statistical confidence. As a consequence, the compute times required for performing the Monte Carlo simulations are very long. This motivated the development of a quasi-analytical method for predicting the success rate of the general algorithm.

The quasi-analytical method is applied to both SIRTf and FAST. The method, which assumes that the algorithm uses the full information contents of a pattern, is analytical except for the fact that it employs two interpolation tables. Because it incorporates conservative approximations and also cannot account for some refinements in the algorithm, the quasi-analytical method yields conservative results.

The sky model used for both test methods is based on the Bahcall and Soneira galaxy model (Bahcall and Soneira, 1980) with extensions based on information from Allen (1976). Fig. 7 shows the assumed integrated star density as a function of the apparent visual magnitude for sky areas of mean, maximum and minimum density. When performing the tests, the log of the density is assumed to be a linear function of magnitude with a slope equal to the value of the faintest guide star used.

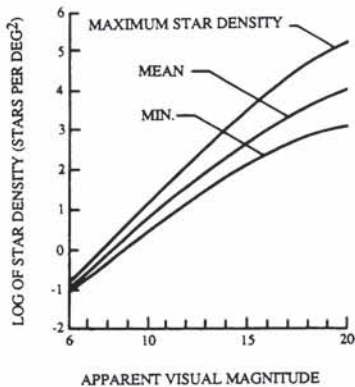


Fig. 7. Integrated Star Density vs Apparent Visual Magnitude for Sky Regions with Maximum, Mean, and Minimum Star Densities.

The parameters used for the Monte Carlo simulations of the SIRTf case (general algorithm, no refinements) are shown in Table 4, while Table 5 lists the parameters employed for the

quasi-analytical evaluation method of both the SIRTf and FAST cases.

TABLE 4 Input Parameters for Simulating the SIRTf Reference Case

PARAMETER				
Group	Description	Symbol	Unit	Value
Sky	10 log of integrated star density at 0 magnitude	A	per square deg	-3.14
	Slope of 10 log star density vs magnitude	B	per magnitude	0.38
Star Catalog	Catalog completeness	CC	fraction	0.95
	Catalog reliability	CR	fraction	0.95
	Magnitude limit		magnitude	15
STR	Radius of field of view	rfov	arcmin	7.5
	Limit to number of observed stars	nosl	per FOV	20
	Dynamic range	mdr	magnitude	5.0
	Sensitivity error	EMMAG	magnitude	0.0
Catalog, STR and Sky	Star position error (1 σ)	epos	arcsec	1.00
	Star magnitude error (1 σ)	EMAG	magnitude	0.45
	Magnitude margin for close disturbing stars	dmd	magnitude	1.75
	Avoidance distance for close disturbing stars	rd	arcsec	9.0
	Clumping factor	fc		3.0
Attitude Error	Pointing error component (1 σ)	epoint	arcmin	5.34
	FOV rotation error (1 σ)	erot	arcmin	5.34
Control Parameters	Tolerance on star magnitude	imag	magnitude	1.16
	Expected relative brightness threshold	THMAG	magnitude	0.67
	Absolute true STR brightness threshold		magnitude	17.0
	Guide star density	ngs	per FOV	9.07
	Tolerance on FOV rotation	trrot	arcmin	17.6
	Tolerance on angle between guide stars	tdis	arcsec	3.78
	Relaxed tolerance on angle between guide stars	tdisl	arcsec	3.78
	Radius of uniqueness area	ru	arcmin	23.75
	Limit to number of stars used for recognition	nbsl		7
	Match confirmation threshold reduction			
	Initial	ICMAXR		1
	Maximum	ICMAXM		5
	Choose best match in case of confusion?			No
	Minimum number of stars in best pattern			3
Program Parameters	Magnitude limit for bright stars	mbi	magnitude	14.8
	Number of evaluations	NEVA		1000

TABLE 5 Input Parameters for Evaluation of Recognition Success Rate of SIRTf and FAST Using the Quasi-Analytical Method

PARAMETER				CASE	
Group	Description	Symbol	Unit	SIRTf Case	Autonomous STR
Sky	Slope of 10 log of star density vs mag	B		0.38	0.45
Star Catalog	Catalog completeness	CC	fraction	0.95	0.95
	Catalog reliability	CR	fraction	0.95	0.95
STR	Limit to number of stars per FOV	nosl		20.0	20.0
	Dynamic range	mdr	magnitude	5.0	5.0
	Sensitivity error	EMMAG	magnitude	0.0	0.0
Catalog, STR and Sky	Star position error (1 σ)	epos	FOV dia	0.0011	0.00025
	Star magnitude error (1 σ)	EMAG	magnitude	0.45	0.30
	Magnitude margin of close disturbing stars	dmd	magnitude	1.75	1.75
	Avoidance of close disturbing stars	rd	FOV dia	0.01	0.01
	Clumping factor	fc		3.0	3.0
	Pointing error (1 σ)	epoint	FOV dia	0.356	n/a
	FOV rotation error (1 σ)	erot	arcmin	5.34	n/a
Control Parameters	Tolerance on star magnitude	imag	magnitude	1.16	0.77
	Expected prob. of meeting mag. tol.	PRMAG	fraction	0.99	0.99
	Expected relative brightness threshold	THMAG	magnitude	0.67	0.42
	Expected prob. of exceeding threshold	PRTH	fraction	0.99	0.99
	Guide star density	ngs	per FOV	9.07	10.0
	Expected prob. of 3 prevald guide stars	PVGS	fraction	0.99	0.995
	Tolerance on FOV rotation	trrot	arcmin	17.6	n/a
	Expected prob. of meeting rotation tol.	PROT	fraction	0.999	n/a
	Relative FOV rotation constraint used?			no	yes
	Tolerance on angle between g.s.'s	tdis	FOV dia	0.0042	0.00091
	Probability of meeting angle tolerance	PDIS	fraction	0.99	0.99
	Uniqueness area	CA	FOV area	10.0	413.0
	Probability FOV in uniqueness area	PIN	fraction	0.99	1.0
	Limit to no. of stars used	nbsl	per FOV	7.0	8.0
Auxiliary Output	True prob. of meeting magnitude tol.	PRMAGT	fraction	0.99	0.99
	True brightness threshold (rel.)	THMAGT	magnitude	0.67	0.42
	True prob. of exceeding bright. threshold	PRTHT	fraction	0.99	0.99
	Density of prevald guide stars	ngs	per FOV	8.43	9.31
	Density of threshold excoeders	nse	per FOV	17.7	16.2
	Probability of 1 star due to dyn. range	DYNF	fraction	0.0123	0.0056
	Fraction of useful stars	prg	fraction	0.84	0.88
Compute Option	Limit to no. threshold excoeders	lte		20.0	20.0
	Method, L (long) or S (short)	L, S		L	L
	Predicted recognition success potential	RSP	fraction	0.966	0.982

Monte Carlo simulations. The Monte Carlo simulation method was developed for evaluating the pattern recognition performance for SIRTf, where the uncertainty area is typically limited to 10 times the size of the STR FOV. Each evaluation (typically 1000 required) involves execution of the following process: First, stars are generated randomly in a field around the expected location of the boresight of the tracker. This field is chosen sufficiently large to ensure that the STR FOV will land inside of it. The mean number of stars in the field depends on the value of the magnitude threshold of the tracker and the magnitude error, while the actual number per evaluation

follows a Poisson distribution based on the aforementioned mean.

The stars are distributed in the field using a uniform distribution, each star is assigned a magnitude consistent with the star density function (parameters A and B of table 4), and the desired number of guide stars (defined by ngs) is selected within the uncertainty area (brightest stars are picked). Next, the STR FOV is placed randomly in the star field, assuming normal distributions for the three attitude errors. This is followed by the assignment of position and magnitude errors to the stars within the STR FOV, assuming normal distributions.

The number of guide stars may be less than desired due to the magnitude limit of the catalog. In addition, some of the brighter stars may not be selected as guide stars, while a number of spurious guide stars are generated, depending upon the defined catalog completeness and reliability. Next, the stars within the STR FOV satisfying the dynamic range constraint and being brighter than the threshold (affected by the STR sensitivity error) are designated as being the observed stars. If their number exceeds the limit to the number used for the recognition ($nbosl$), then the brightest $nbosl$ stars are selected for use in the recognition process.

An observed guide star will be disqualified if there is a disturbing star within a distance rd of it, where rd depends on the point spread function, which will be a function of the pixel size of the detector. A star is deemed disturbing if it is within the avoidance distance rd , and not at least dmd magnitude fainter than the observed guide star. In order to account for the fact that the stars are in reality not uniformly distributed but tend to be grouped in binary and multiple systems, the mean star density within an area with radius rd around each observed guide star can be biased using the clumping factor fc . An fc factor of three triples the local star density and thus the probability of the presence of a disturbing star.

In addition to the control parameters mentioned, the size of the uncertainty area (ru), and the mode of the algorithm (choose best match in case of ambiguity?, ISWPR in Fig. 5) need to be defined. Next, the recognition algorithm is applied and the result is obtained. Following each evaluation, the recognition statistics are updated and diagnostic output is generated for each evaluation resulting in a recognition failure.

Quasi-analytical method. The objective of the quasi-analytical method is to predict the recognition success rate for algorithms using the full information contents of a pattern. The method, which uses the same input parameters as the Monte Carlo simulations, computes the recognition success probability by solving the following equation:

$$RSP = PROT \sum_{i=2}^{\infty} PTE(i) \sum_{j=2}^{\infty} PDL(i, is) \sum_{k=2}^{\infty} PPVR(i, is, j) \sum_{k=2}^{\infty} PVR(j, k) PSR(i, is, k)$$

where $PROT$ is the probability that the FOV rotation is less than the tolerance (for the FAST case this is 1), $PTE(i)$ is the probability that i stars within the STR FOV exceed the brightness threshold of the STR, and $PDL(i, is)$ is the probability of having is observed stars available for recognition, given i threshold exceders. The PDL distribution depends on the dynamic range of the STR and the limit to the number of observed stars used for the recognition process (is is limited to this number). $PPVR(i, is, j)$ is the probability of having j observed guide stars with a magnitude error less than the magnitude tolerance among the is observed stars used for the recognition, given i threshold exceders. $PVR(j, k)$ is the probability that a pattern of k of the aforementioned j observed guide stars satisfies the geometrical conditions imposed by the recognition algorithm, i.e., k of the j stars are valid observed guide stars. Finally, the quantity $PSR(i, is, k)$ is the probability of successful recognition if k of the observed stars used for recognition are valid observed guide stars, given a total of i threshold exceders.

Since the value of $PSR(i, is, k)$ depends, among other things, on the geometry of the star pattern, this distribution cannot be generated using analysis. Instead, the distribution is obtained

using an interpolation table that was generated using Monte Carlo simulations. The distribution $PVR(j, k)$ also depends on the geometry of the pattern, and a look-up table is used to generate this distribution. Monte Carlo simulations were also used to create this look-up table. The details of the quasi-analytical method, including a description of how the probability distributions depend on the input parameters, have been presented in a paper by van Bezooijen (1986).

The quasi-analytical method has been implemented in an interactive computer program. The method permits the control parameters to be specified either directly or in terms of a probability associated with it, as is shown in Table 5. If the second option is selected, which usually makes more sense, the program computes the value of the control parameter.

Space Infra Red Telescope Facility Case

Simulation of the SIRTf reference case, specified by the parameter values shown in Table 4, showed that in a sky area with mean star density the base recognition algorithm successfully identified the stars in 968 of the 1000 evaluations. Line number 3 of Table 6, which pertains to this case, gives an assessment of the failed cases. In only one of the 1000 cases, the algorithm assumed a successful recognition while in reality it was a failure, which demonstrates the robustness of the algorithm. Two of the three unrecognized failures would have resulted in correct attitudes. They were deemed failures because one of the stars in a large pattern was incorrectly identified. Thirteen failures were caused by the dynamic range limiting the number of observable stars to just one. Of the 16 remaining failures, the failure causes include lack of a sufficient number of valid observed guide stars (not enough guide stars and guide stars with out of tolerance magnitude or position errors), and lack of uniqueness of the pattern of observed guide stars.

TABLE 6 Pattern Recognition Success Rate for SIRTf as Predicted by Monte Carlo Simulations

Limit to Number of Obs. Stars Used	Select Best Match ?	Star Magnit. Tolerance	Relaxed Distance Tolerance	Successes (out of 1000)	Failures		
					Unrecognized	Dynamic Range Problem	Other
					Okay * True		
3	No	1.16	3.78	921	1	1	13
5	No	1.16	3.78	966	3	2	13
7	No	1.16	3.78	968	2	1	13
10	No	1.16	3.78	973	3	2	13
3	Yes	1.52	4.67	950	2	3	13
5	Yes	1.52	4.67	967	4	1	13
7	Yes	1.52	4.67	975	3	1	13
10	Yes	1.52	4.67	977	4	1	13

* Attitude computed correctly.

By comparing line 7 with line 3 of Table 6, it may be seen that the number of successful cases (including okay failures) is raised from 970 to 978 by using a larger magnitude tolerance and implementation of two refinements: a relaxed angular distance tolerance, and selection of the best match in case of ambiguity. Table 6 also shows how the performance is effected by the limit to the number of observed stars used for the recognition process. A low value of this limit allows a software reduction and the use of a simpler tracker at the cost of a reduction in performance.

It was found that use of the special algorithm resulted in a successful recognition for 975 of the 1000 evaluations, instead of the 970 successes for the base general algorithm and the 978 successes obtained with the refined general algorithm. This performance is quite good considering the significant reduction in software that its use permits.

Fig. 8 compares the recognition success probability predictions as obtained with the quasi-analytical method with those generated by the Monte Carlo simulations (assuming use of the base general algorithm) for three sky areas. The success rate is shown as a function of the limit to the number of observed stars used for the recognition. The filled in circles refer to simulation cases involving 5000 evaluations, while the open circles were generated using 1000 evaluations per case. Although slightly conservative, the quasi-analytical method matches the

simulation results very well, and correctly predicts a reduction in performance with an increase of the limit to the number of observed stars used. This is due to the fact that as this limit is increased, the fraction of guide stars among the observed stars is reduced, causing a reduction of the uniqueness probability of the pattern of observed guide stars.

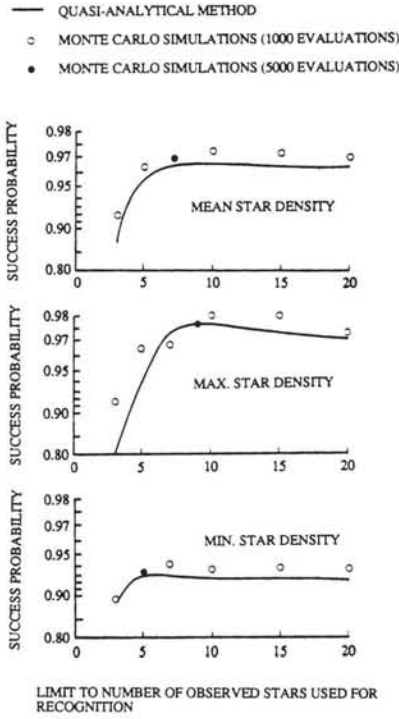


Fig. 8. Star Pattern Recognition Success Probability as Predicted Using the Quasi-Analytical Method and as Obtained Through Monte Carlo Simulations.

Whereas the Monte Carlo simulations (5000 evaluations) require a compute time ranging from 250 to 510 minutes (respectively for sky areas with minimum and maximum star densities), the quasi-analytical method yields practically the same results in a mere 0.6 to 1.8 minutes. The success rate is different for the different sky areas due to the fact that the star catalog is insufficiently deep at the galactic poles, limiting the guide star density to 6.7 stars per STR FOV. In addition, the performance also depends on the A and B parameters characterizing the sky, which are -3.96 and 0.5 for the sky area with maximum density (case 2), while for the area with minimum density (case 3) the values are -2.37 and 0.30 .

Finally, it is worth mentioning that the recognition success probability for cases like SIRTf can be increased to practically 100% by performing two or three independent recognition attempts in adjacent parts of the sky at the cost of some slew time.

Full-sky Autonomous Star Tracker Case

The FAST that is evaluated using the quasi-analytical method has a circular FOV with an area of 100 square degrees, an accuracy of 10 arcsec (1σ) relative to a detector attached coordinate system, a dynamic range of 5 magnitudes, uses a guide star density of 10 stars per FOV, and needs to be sufficiently sensitive to observe stars with a magnitude of 7.5. Table 5 shows the parameters used for FAST. Since the FOV is 100 square degrees, it follows that the size of the uncertainty area is 413 times that of the tracker FOV. Since the guide stars are fairly bright, it is appropriate to assume a magnitude error of 0.3 (1σ). It turned out to be optimum to limit the number of observed stars used for recognition to the brightest 8. Hence, the FAST needs to adjust its threshold to a value where 8 stars are observed, unless this is prevented by the dynamic range constraint of the tracker.

A FAST with these parameters is expected to have a recognition success probability of 98.2%. If the dynamic range were increased to 10 magnitudes, the success rate would go up to 99.3%. Hence, of the 1.8% failure rate, 1.1% can be attributed to the dynamic range constraint of the tracker. Since successful recognition requires at least 3 guide stars within the FOV, while a significant fraction of cases with three guide stars will fail, it is important to note that the probability of having less than 3 guide stars is 0.28%, while the probability of having 3 guide stars is 0.76%. This is true because the quasi-analytical method assumes a Poisson distribution for the number of guide stars within the FOV. Hence, the percentage of failures due to a lack of guide stars is expected to be in the range from 0.28 to 1.04%. Therefore, virtually all failures can be attributed either to the dynamic range constraint of the tracker or to the absence of a sufficient number of guide stars within the STR FOV.

Since ASTROS II has the dynamic range and sensitivity mentioned for FAST, is expected to have a better accuracy (8 instead of the 10 arcsec), and has a larger FOV area (circular field inscribed in the square 11.5 by 11.5 degrees FOV covers 100 square degrees), an ASTROS II based FAST is expected to exhibit a success rate of at least 98.2%.

COMPUTATIONAL REQUIREMENTS FOR FAST

The memory required for FAST has been computed assuming use of ASTROS II. Since the algorithm consists of only approximately 500 lines of Fortran source code, the memory required for storing the code is negligible. To compute the amount of memory space required, it is necessary to know the number of guide stars, the upper limit of the match confirmation value, and the number of guide star pairs. In order to limit the number of guide star pairs, it is best to only use that part of the ASTROS II FOV that lies within the circle inscribed within the square FOV. This implies that the useful part of the FOV measures some 100 square degrees, which requires the use of 4,125 guide stars assuming a guide star density of 10 stars per FOV.

Each guide star has a number of guide star neighbors within a distance equal to the diameter of the STR FOV that averages 4 times the guide star density. Hence, the total number of guide star pairs is approximately equal to the product of 4 times the guide star density and the number of guidestars divided by two. This implies that the number of guide star pairs with angular distance less than the FOV diameter is approximately 82,500. Using 2 byte integers, it takes a total of 6 bytes per pair to specify the angular distance and to identify the guide stars associated with each pair, resulting in a total of 495,000 bytes.

Since the integrated probability versus the angular distance of the guide star pairs and the observed star pairs are quadratic functions, it follows that, on the average, the number of guide star pairs matching a pair of observed star pairs is equal to $4/3$ times twice the distance tolerance times the total number of guide star pairs. Hence, assuming a distance tolerance equal to $8/10$ times 0.00091 (8 arcsec accuracy instead of 10), it follows that on the average, each observed star pair matches the angular distance of 160 guide star pairs.

For the magnitude tolerance used (0.77) and the slope of the log of the integrated star density (0.45), the probability of a guide star matching the brightness of an observed star can be found to be less than 0.55. Hence, the probability of both stars of a guide star pair matching the brightness of the stars of the observed star pair is equal to 0.3 for each of the two orientations of the guide star pair relative to the observed star pair. This implies that the number of star matches resulting from a guide star pair matching the angular distance of an observed star pair is equal to $2 \times 0.3 \times 2 = 1.2$.

Since the number of observed stars used for the recognition process is limited to 8, the maximum number of observed star pairs is equal to 28. Therefore, the upper limit for the number of star matches is estimated at $1.2 \times 28 \times 160 = 5376$. From simulations it was found that spurious matches can increase the confirmation value from 7 to 11. Hence, matrix $MAT(ig,j)$ and its copy measure $5376 \times 11 \times 2 = 118,272$ bytes each. Since these matrices are very sparse, it is possible to replace each by a

number of smaller matrices reducing the memory space by a factor of 2.8.

This brings the memory space for the guide star pairs and the MAT matrices to 579,480 bytes. Since these matrices represent roughly 70% of the space needed, it follows that the total amount of memory space is approximately 810K bytes. It is preferable to store the guide star pairs and the code in (P)ROM.

Assuming fixed point arithmetic and the use of a MC68000 class microprocessor operating at 12 Mhz with no wait states, it can be shown that generation of the base match matrices will take approximately 0.55 s. The additional time required for performing the recognition is estimated at 0.1 s, resulting in a total time of approximately 0.65 s.

Since most of the compute time is required for the star matching process used for generating the base match matrices, it follows that the compute time depends mainly on the spatial accuracy of FAST. For example, an increase of the spatial error from 8 to 40 arcsec would result in roughly a five fold increase in recognition time. In addition, the memory space required for the MAT matrices would increase five fold, resulting in an increase of the total memory space required by approximately 1300K bytes. Furthermore, this reduction in accuracy would reduce the recognition success rate by 0.35%.

In summary, the memory space required for a FAST based on ASTROS II is estimated at 810K bytes, while the compute time is expected to be less than 1 s, assuming the ASTROS II microprocessor to be as fast as the MC68000 at 12 Mhz. Both the fast compute time and the manageable amount of memory are enabled by the high spatial accuracy of the tracker.

CONCLUSIONS

Using the general star pattern recognition algorithm described in this paper, JPL's redundant, microcomputer equipped ASTROS II CCD star tracker could be developed into a Full-sky Autonomous Star Tracker (FAST), capable of determining its attitude about all three axes without requiring any a-priori attitude knowledge. This would allow ASTROS II to be integrated as a key sensor in future autonomous attitude control and navigation systems.

Having an 11.5 by 11.5 field of view and an accuracy of 8 arcsec (1 sigma, goal), an ASTROS II based FAST requires the use of approximately 4,100 guide stars, necessitating a memory of 810K bytes. With space qualified 256 K bit ROM and RAM chips becoming available in the near future, this amount of memory can be provided by less than 50 memory chips (including EDAC). The SA 3300 microprocessor of ASTROS II is expected to be capable of performing the attitude determination in approximately one second.

An ASTROS II based FAST is expected to have a 98.2% success rate in predicting its attitude. The 1.8% failure rate is almost completely due to the dynamic range limitation of the tracker (assumed to be 5 magnitudes) and a lack of observed guide stars (Poisson distribution assumed). The former effect results in a failure rate of 1.1%, while the latter is responsible for most of the remaining 0.7%. This implies that the star pattern recognition algorithm is virtually 100% effective. Furthermore, the algorithm is very robust in the sense that the probability of false star pattern recognition, and thus erroneous attitude determination, is negligible.

Using both Monte Carlo simulations and a quasi-analytical method, it was shown that the general recognition algorithm and a less software intensive special algorithm, can be used to reliably automate the acquisition of celestial targets by astronomy telescopes (e.g., SIRTIF for which the method was tested). This function is currently often performed by a human operator.

In addition to enabling the construction of a FAST and automating the acquisition of celestial targets by astronomy telescopes, the recognition algorithm can also be used for autonomous updating of gyro based attitude control systems (as is planned for Mariner Mark II), and for automating ground based attitude reconstruction.

JPL is currently applying neural network technology to the problem of autonomous star pattern recognition with some encouraging early results.

ACKNOWLEDGEMENTS

The author gratefully acknowledges the NASA Ames Research Center and the Jet Propulsion Laboratory, California Institute of Technology, for their partial support of the research described in this paper under contract with the National Aeronautics and Space Administration. He also would like to thank Professor J.D. Powell of Stanford University, Dr. K.R. Lorell of Lockheed Palo Alto Research Laboratory, and Dr. E.W. Dennison of the Jet Propulsion Laboratory for their help and advice on the star pattern recognition research.

REFERENCES

- Allen, C.W. (1976). *Astronomical Quantities*, 3rd ed. The Athlone Press, University of London, London.
- Bahcall, J.N., and R.M. Soneira (1980). The universe at faint magnitudes: I. Models for the Galaxy and the predicted star counts. *The Astrophysical Journal Supplement Series*, Vol 44, pp 73-110.
- Christis, W.J. (1974). The optical sensors of the Netherlands Astronomical Satellite (ANS), the star sensor, *Philips Tech. Rev.*, Vol 34, pp 218-224.
- Dennison, E.W., R.H. Stanton, and K. Shimada (1987). The development of a Charge-Coupled Device tracker for spacecraft. Paper AAS 87-007, 10th Annual AAS Guidance and Control Conference, Keystone, Colorado, Feb 1987.
- Draper, R.F. (1988). The Mariner Mark II Program. Paper AIAA 88-0067, AIAA 26th Aerospace Sciences Meeting, Reno, Nevada, Jan 1988.
- Eisenhardt, P., and G.G. Fazio (1988). The SIRTIF concept and its realization. NASA Ames Research Center, Moffett Field, CA, Nov 17, 1988.
- Junkins, J.T., and T.E. Strikwerda (1979). Autonomous star sensing and attitude estimation. Paper AAS 79-013, Annual AAS Guidance and Control Conference, Keystone, Colorado.
- Lasker, B.M., H. Jenker, and J.L. Russell (1987). The guide star catalog. Proceedings of IAU Colloquium No. 133, Paris, France, June 1987.
- McLaughlin, W.I., and W.H. de Leeuw (1978). Infrared Astronomical Satellite. *Spaceflight*, Vol 20, pp 187-191, May 1978.
- Rhoads Stephenson, R. (1985). The Galileo attitude and articulation control system: a radiation-hard, high-precision, state-of-the-art control system. Tenth IFAC symposium on automated control in space, Toulouse, France, June 1985.
- van Bezooijen, R.W.H. (1977). IRAS attitude control subsystem. ESA SP-128, pp 187-191, Nov 1977.
- van Bezooijen, R.W.H., K.R. Lorell, and J.D. Powell (1985). Automated star pattern recognition for use with the Space Infrared Telescope Facility (SIRTIF). Tenth IFAC symposium on automated control in space, Toulouse, France, June 1985.
- van Bezooijen, R.W.H. (1986). Success potential of automated star pattern recognition. Paper AIAA-86-0254, AIAA 24th Aerospace Sciences Meeting, Reno, Nevada, Jan 6-9, 1986.
- Wong, E.C., and W.G. Breckenridge (1983). Inertial attitude determination for a dual-spin planetary spacecraft. *AIAA J. of Guidance, Control, and Dynamics*, pp 491-498.